DALTON
FULL PAPER

Synthesis and characterisation of triosmium nitrite clusters containing phosphine ligands

Bernard Kwok-Man Hui and Wing-Tak Wong *

Department of Chemistry, The University of Hong Kong, Pokfulam Road, Hong Kong, P. R. China

The nitrite cluster $[Os_3(\mu\text{-H})(CO)_{10}(\mu\text{-}\eta^2\text{-}NO_2)]$ **1** reacted with trimethylamine *N*-oxide in CH_2Cl_2 to give a pair of isomers with formula $[Os_3(\mu\text{-H})(CO)_9(\mu\text{-}\eta^2\text{-}NO_2)(NMe_3)]$ **2a** and **2b** in moderate yields. Reaction of **1** with PPh_3 and Me_3NO in CH_2Cl_2 gave a pair of isomers $[Os_3(\mu\text{-H})(CO)_9(\mu\text{-}\eta^2\text{-}NO_2)(PPh_3)]$ **3a** and **3b** and $[Os_3(\mu\text{-H})(CO)_8(\mu\text{-}\eta^2\text{-}NO_2)(PPh_3)_2]$ **4**. With *cis*-1,2-bis(diphenylphosphino)ethylene (dppen) and Me_3NO in CH_2Cl_2, **1** gave a pair of isomers $[Os_3(\mu\text{-H})(CO)_8(\mu\text{-}\eta^2\text{-}NO_2)(dppen)]$ **5a** and **5b**, and $[Os_3(\mu\text{-H})(CO)_6(\mu\text{-}\eta^2\text{-}NO_2)(dppen)_2]$ **6**. Reaction of **1** with bis(diphenylphosphino)acetylene (dppa) and Me_3NO in CH_2Cl_2 gave $[Os_3(\mu\text{-H})(CO)_8(\mu\text{-}\eta^2\text{-}NO_2)(dppa)]$ **7** in good yield. The dppa co-ordinates to two Os atoms to form a six-membered ring suffering from severe angle strain in which the carbon–carbon triple bond is maintained. All the products were characterised by IR, NMR and FAB mass spectroscopies. All these clusters contain an asymmetrically bridging NO_2^- ligand along one Os–Os edge of the triosmium metal framework, as is evident from structural determinations of **2a**, **2b**, **3b**, **4**, **5a**, **6** and **7**.

The co-ordination chemistry of nitrite ligands toward various metal centres such as Co, Ni, Cu, Pd, Pt and Re is well documented.[1–9] Examples of triosmium nitrite clusters are much scarcer and their chemistry is not well known. Recently, we have reported the synthesis and characterisation of the triosmium nitrite complexes $[N(PPh_3)_2][Os_3(CO)_{10}(\mu\text{-}\eta^2\text{-}NO_2)]$ and $[Os_3(\mu\text{-H})(CO)_{10}(\mu\text{-}\eta^2\text{-}NO_2)]$ **1**.[10] We believe that the presence of an electron-withdrawing NO_2^- group on the cluster framework should produce a pronounced effect on the cluster reactivity and that this should be reflected by the ligand addition and substitution reactions. The chemistry of phosphine ligands with triosmium carbonyl clusters is well developed,[11–18] but there are no similar studies on triosmium nitrite complexes. The presence of phosphine ligands on the triosmium nitrite clusters may affect the subsequent ligand transformations and rearrangements. Thus, the reactivity of triosmium nitrite clusters with phosphine ligands is one of our current interests. In this paper the synthesis and characterisation of some triosmium nitrite complexes with a number of phosphine ligands, triphenylphosphine, *cis*-1,2-bis(diphenylphosphino)ethylene and bis(diphenylphosphino)acetylene, is reported.

Results and Discussion

The reaction of $[Os_3(\mu\text{-H})(CO)_{10}(\mu\text{-}\eta^2\text{-}NO_2)]$ **1** with trimethylamine *N*-oxide (Me_3NO) in CH_2Cl_2 at room temperature gave two isomers of formula $[Os_3(\mu\text{-H})(CO)_9(\mu\text{-}\eta^2\text{-}NO_2)(NMe_3)]$ **2a** and **2b** in moderate yields, see Scheme 1. The spectroscopic data of these two isomers were very similar (Table 1) and were fully consistent with their molecular structures determined by single-crystal X-ray analysis. Both isomers undergo gradual decomposition over 1 d under ambient conditions.

The molecular geometry of complex **2a** is illustrated in Fig. 1 and selected bond lengths and angles are given in Table 2, while the other isomer **2b** is illustrated in Fig. 2 with selected bond parameters in Table 3. The molecular geometries of the complexes are similar but differ in the disposition of the co-ordinated NMe_3 groups to the triosmium core. The bond parameters of the $Os_3(NO_2)$ core are very similar and the Os–NMe_3 distances [2.27(2) Å] are identical with experimental errors. Osmium carbonyl clusters containing trimethylamine were proposed as intermediates in many substitution chemical

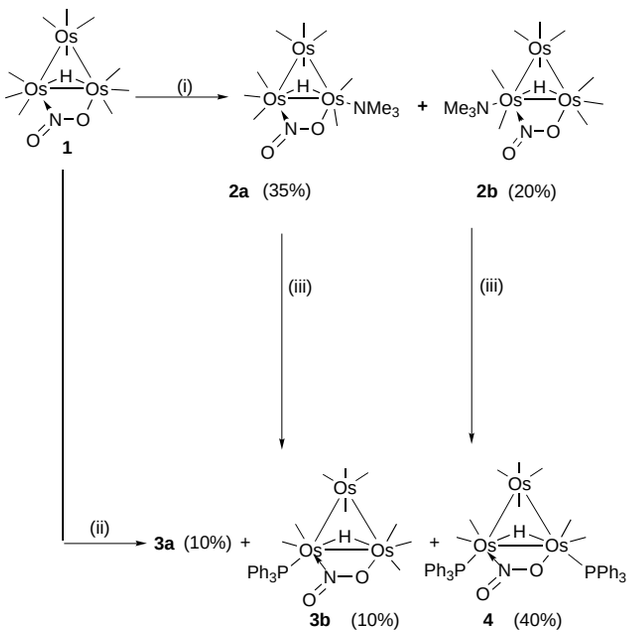

Scheme 1 (i) Me_3NO, CH_2Cl_2, room temperature; (ii) excess of PPh_3, Me_3NO, CH_2Cl_2 at 40 °C; (iii) excess of PPh_3, Me_3NO, CH_2Cl_2 at 40 °C

reactions involving the use of Me_3NO. However, structurally established examples are relatively rare.[19–21] Both isomers **2a** and **2b** have a bridging hydride (δ −10.7 and −10.4 respectively) and a bridging NO_2^- ligand bonded onto the same Os(1)–Os(2) edge *via* N(1) and O(10) [Os(2)–N(1) 2.10(2), Os(1)–O(10) 2.13(2) and Os(2)–N(1) 2.06(2), Os(1)–O(10) 2.17(2) Å respectively]. These values are similar to those measured in **1** [2.11(2) and 2.13(1) Å].[10] The dihedral angle between the planes defined by the osmium triangle and the nitrite ligand in **2a** and **2b** is 103.1 and 95.0° respectively. The uneven electron distribution from the asymmetrically bridging nitrite ligand onto the two osmium atoms affects the strength of π back bonding to their adjacent carbonyl groups and this difference in CO stretching can be observed from their IR spectra (Table 1). This will also affect the ease of substitution of these CO groups. It also appears that cluster **2a** is more thermodynamically

Table 1 Spectroscopic data for compounds **2a**–**7**

Compound	IR $\tilde{\nu}$(CO)[a]/cm^{-1}	^{1}H NMR δ(*J*/Hz)[b]	^{31}P NMR δ[c]	Mass spectrum[d] *m*/*z*
2a	2105w, 2067s, 2027s, 2010s, 1999m and 1933w	−10.7 (s, 1 H, OsH), 3.0 (s, 3H, NCH_3)	—	929 (929)
2b	2104m, 2064s, 2022s, 2007s, 1982w and 1951w	−10.4 (s, 1 H, OsH), 3.2 (s, 3 H, NCH_3)	—	929 (929)
3a	2102s, 2066s, 2026s, 2011s, 1977w and 1953w	7.5–7.4 (m, 15 H, Ph), −11.2 (d, 1 H, J_{PH} 11.1, OsH)	19.5 (s)	1132 (1132)
3b	2101, 2062s, 2027s, 2014s and 1981m	7.5–7.3 (m, 15 H, Ph), −11.3 (d, 1 H, J_{PH} 11.0, OsH)	10.6 (s)	1132 (1132)
4	2080s, 2018s, 2010s, 1968m and 1943m	7.5–7.4 (m, 30 H, Ph), −10.1 (d, 1 H, J_{PH} 2.4, OsH)	17.4 (s), 11.0 (s)	1367 (1366)
5a	2082m, 2051w, 2014s, 1997s and 1964w	7.5–7.3 (m, 20 H, Ph), −12.4 (d, 1 H, J_{PH} 15.5, OsH)	−15.3 (s), −13.7 (s)	1238 (1238)
5b	2064m, 2009w, 1988s and 1950w	7.4–7.2 (m, 20 H, Ph), −10.9 (d, 1 H, J_{PH} 7.1, OsH)	51.0 (s), 45.9 (s)	1238 (1238)
6	2064w, 2040w, 2003s, 1960m and 1927m	7.6–7.4 (m, 20 H, Ph), 7.3–6.9 (m, 20 H, Ph), −8.4 (m, 1 H, OsH)	50.1 (s), 49.1 (s), 38.1 (s), 30.5 (s)	1580 (1579)
7	2088s, 2016s, 1975m and 1953m	7.8–7.5 (m, 20 H, Ph), −7.4 (m , 1 H, OsH)	35.6 (s), 28.5 (s)	1237 (1236)

[a] In CH_2Cl_2. [b] In $CDCl_3$ with $SiMe_4$ as internal reference. [c] In $CDCl_3$ with 85% H_3PO_4 as internal reference. [d] Positive FAB; simulated values in parentheses.

Table 2 Selected bond lengths (Å) and angles (°) for compound **2a**

Os(1)–Os(2)	2.937(1)	Os(1)–Os(3)	2.820(2)
Os(2)–Os(3)	2.856(2)	Os(1)–N(2)	2.27(2)
Os(1)–O(10)	2.13(2)	Os(2)–N(1)	2.10(2)
O(10)–N(1)	1.35(2)	O(11)–N(1)	1.20(2)
Os(1)–Os(2)–Os(3)	58.2(3)	Os(1)–Os(3)–Os(2)	62.3(4)
Os(2)–Os(1)–Os(3)	59.5(3)	Os(1)–O(10)–N(1)	108(1)
Os(2)–Os(1)–O(10)	69.1(4)	Os(2)–Os(1)–N(2)	108(1)
Os(2)–N(1)–O(10)	115(1)	Os(2)–N(1)–O(11)	127(1)
O(10)–N(1)–O(11)	116(1)		

Table 3 Selected bond lengths (Å) and angles (°) for compound **2b**

Os(1)–Os(2)	2.911(2)	Os(1)–Os(3)	2.839(2)
Os(2)–Os(3)	2.836(2)	Os(1)–O(10)	2.17(2)
Os(2)–N(2)	2.27(2)	Os(2)–N(1)	2.06(2)
O(11)–N(1)	1.21(3)	O(10)–N(1)	1.33(2)
Os(1)–Os(2)–Os(3)	59.20(4)	Os(1)–Os(3)–Os(2)	61.73(4)
Os(2)–Os(1)–Os(3)	59.07(4)	Os(1)–Os(2)–N(1)	66.1(6)
Os(1)–Os(2)–N(2)	110.4(6)	Os(1)–O(10)–N(1)	103(1)
Os(2)–Os(1)–O(10)	69.6(5)	Os(2)–N(1)–O(10)	120(1)
Os(2)–N(1)–O(11)	129(2)	O(10)–NM(1)–O(11)	108(2)

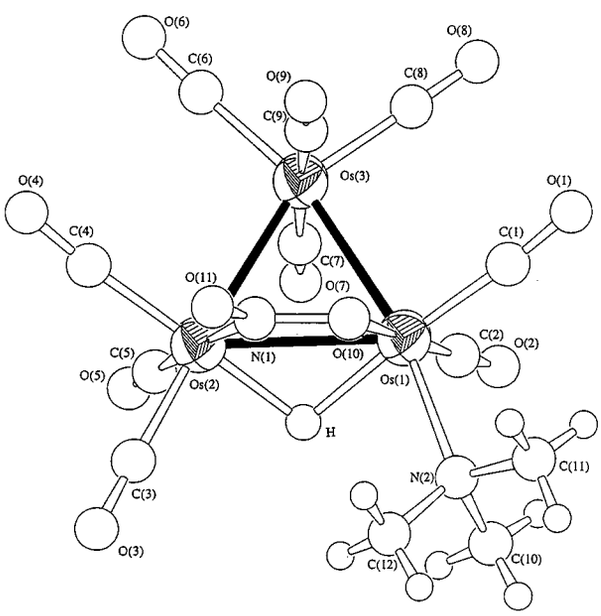

Fig. 1 Molecular structure of $[Os_3(\mu\text{-H})(CO)_9(\mu\text{-}\eta^2\text{-}NO_2)(NMe_3)]$ **2a**

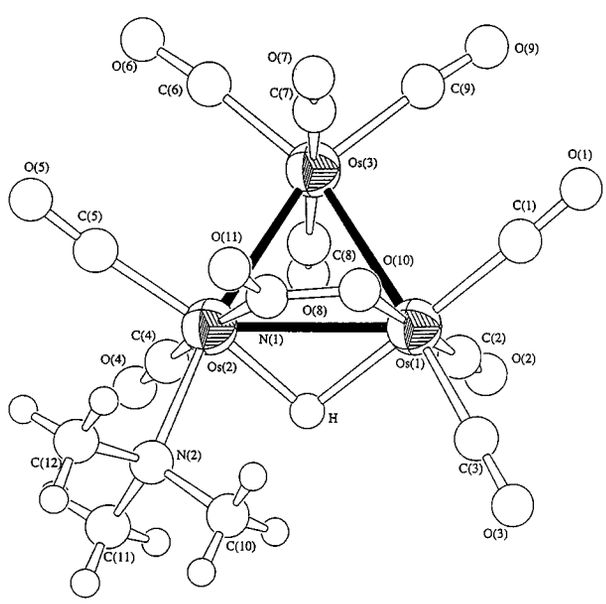

Fig. 2 Molecular structure of $[Os_3(\mu\text{-H})(CO)_9(\mu\text{-}\eta^2\text{-}NO_2)(NMe_3)]$ **2b**

favourable based on steric considerations, consistent with the observation of a higher yield for cluster **2a** (35%) than that of **2b** (20%). In contrast to the substitutions of many other well established cluster systems $[Os_3(\mu\text{-H})(\mu\text{-X})(CO)_{10}]^{2-}$[22–25] (X = 3e$^-$ donor) this nitrite cluster allows a study of the selectivity of substitution of CO.

Since the NMe_3 group in complexes **2a** and **2b** is substitution labile, we believe that substitution reactions on the osmium frameworks take place readily in the presence of strong nucleophiles such as phosphine ligands. While monosubstitutions are to be expected, disubstitution of the phosphine ligands may also be feasible.

Reaction of complex **1** with Me_3NO in the presence of an excess of triphenylphosphine afforded a pair of isomers with formula $[Os_3(\mu\text{-H})(CO)_9(\mu\text{-}NO_2)(PPh_3)]$ **3a** and **3b**, and $[Os_3(\mu\text{-H})(CO)_8(\mu\text{-}NO_2)(PPh_3)_2]$ **4** based on spectroscopic evidence (Scheme 1). Proton and ^{31}P NMR spectroscopies indicated that, in all cases, the hydride ligand remains incorporated with the cluster core and co-ordination of the phosphine ligands was observed. In order unambiguously to establish their molecular

Table 4 Selected bond lengths (Å) and angles (°) for compound **3b**

Os(1)–Os(2)	2.9062(8)	Os(1)–Os(3)	2.8491(8)
Os(2)–Os(3)	2.8830(8)	Os(1)–O(10)	2.123(1)
Os(2)–P	2.393(4)	Os(2)–N	2.09(1)
O(10)–N	1.30(1)	O(11)–N	1.22(1)
Os(1)–Os(2)–Os(3)	58.96(2)	Os(1)–Os(3)–Os(2)	60.92(2)
Os(2)–Os(1)–Os(3)	60.11(2)	Os(1)–Os(2)–N	67.4(3)
Os(1)–Os(2)–P	119.60(9)	Os(2)–Os(1)–O(10)	67.8(3)
Os(1)–O(10)–N	110.4(8)	Os(2)–N–O(10)	114.4(9)
Os(2)–N–O(11)	131(1)	O(10)–N–O(11)	114(1)

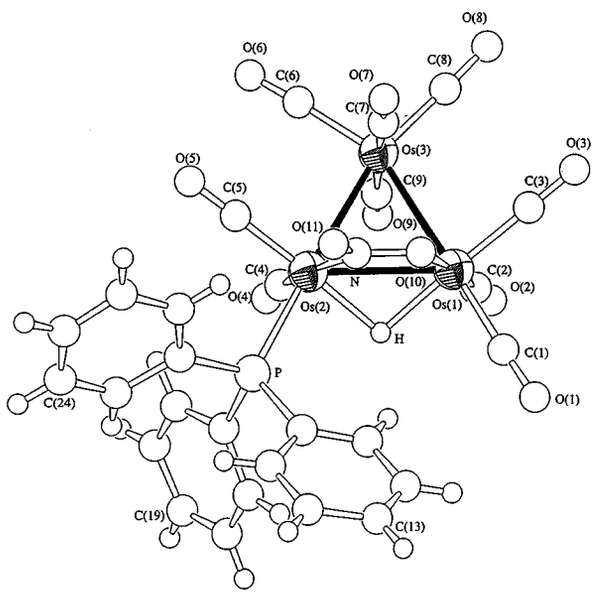

Fig. 3 Molecular structure of $[Os_3(\mu\text{-}H)(CO)_9(\mu\text{-}\eta^2\text{-}NO_2)(PPh_3)]$ **3b**

structures, single-crystal X-ray analyses were carried out for **3b** and **4**.

The molecular structure of complex **3b** is illustrated in Fig. 3 and pertinent bond parameters are given in Table 4. The Os(1)–Os(2) edge, as observed in **1**, is doubly supported by the nitrite ligand [Os(2)–N 2.09(1) and Os(1)–O(10) 2.123(1) Å] and the hydride ligand. The N–O bond distances in the NO_2^- moiety are O(10)–N 1.30(1) and O(11)–N 1.22(1) Å. The PPh_3 ligand is bound to the cluster [Os(2)–P 2.393(4) Å] in the equatorial position. This relatively bulky substituent leads to a larger Os(1)–Os(2)–P angle [119.60(9)°] than the corresponding Os(1)–Os(2)–N(2) angle [110.4(6)°] in **2b**. In addition, a larger dihedral angle was found between the osmium triangle and the plane containing the nitrite ligand (103.1°) compared to that observed in **2b** (95.0°).

The positive FAB mass spectra of complexes **3a** and **3b** showed an identical molecular ion peak and hence suggested that they are isomeric but again differ in the disposition of the PPh_3 ligand on the cluster core, as manifested by **2a** and **2b**. However, single crystals of **3a** suitable for structural analysis could not be obtained. It is believed that complexes **2a** and **2b** reacted with triphenylphosphine separately to afford cluster **3a** and **3b** respectively (Scheme 1). There is no spectroscopic evidence supporting interconversions between clusters **2a** and **2b** or **3a** and **3b**.

The molecular structure of complex **4** is illustrated in Fig. 4 and selected bond lengths and angles are given in Table 5. We believe that both **3a** and **3b** are the precursors that reacted further with the excess of triphenylphosphine in the presence of trimethylamine *N*-oxide to afford complex **4**. The two PPh_3 ligands are terminally co-ordinated to the cluster *via* P(1) [Os(1)–P(1) 2.379(5)] and P(2) [Os(2)–P(2) 2.379(5) Å] and are arranged equatorially so that steric interaction between them is

Table 5 Selected bond lengths (Å) and angles (°) for compound **4**

Os(1)–Os(2)	2.946(1)	Os(1)–Os(3)	2.860(1)
Os(2)–Os(3)	2.868(1)	Os(1)–P(1)	2.379(5)
Os(2)–P(2)	2.379(5)	Os(2)–N	2.11(2)
Os(1)–O(9)	2.13(2)	O(9)–N	1.36(2)
O(10)–N	1.25(3)		
Os(1)–Os(2)–Os(3)	58.92(3)	Os(1)–Os(3)–Os(2)	61.90(3)
Os(2)–Os(1)–Os(3)	59.18(3)	Os(1)–Os(2)–P(2)	120.8(1)
Os(1)–Os(2)–N	66.1(4)	Os(2)–Os(1)–O(9)	69.7(4)
Os(2)–Os(1)–P(1)	120.8(1)	Os(2)–N–O(10)	136(1)
Os(2)–N–O(9)	116(1)	Os(1)–O(9)–N	107(1)
O(9)–N–O(10)	106(1)		

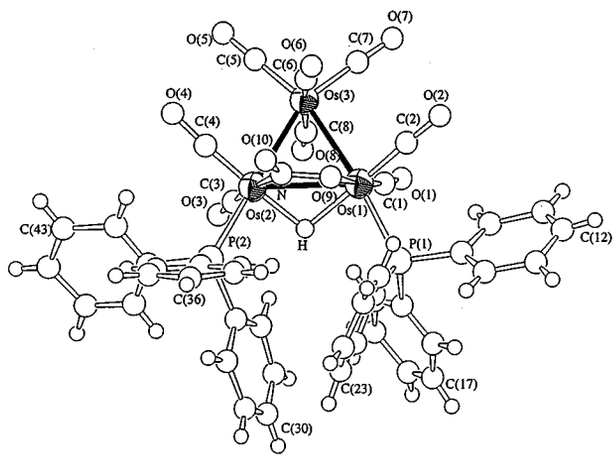

Fig. 4 Molecular structure of $[Os_3(\mu\text{-}H)(CO)_8(\mu\text{-}\eta^2\text{-}NO_2)(PPh_3)_2]$ **4**

minimised. Nonetheless, a significantly longer Os(1)–Os(2) distance is observed [2.946(1) Å] compared to the corresponding distance [2.9062(8) Å] in **3b**. Two phosphorus signals were recorded at δ 17.4 and 11.0 in the ^{31}P NMR spectrum. In the ^1H NMR spectrum the hydride is at δ −10.1, bridging the Os(1)–Os(2) edge.

The reaction of complex **1** with the bidentate ligand *cis*-1,2-bis(diphenylphosphino)ethylene (dppen) and Me_3NO in CH_2Cl_2 gave a pair of isomers with formula $[Os_3(\mu\text{-}H)(CO)_8(\mu\text{-}\eta^2\text{-}NO_2)(dppen)]$ **5a** and **5b**, and $[Os_3(\mu\text{-}H)(CO)_6(\mu\text{-}\eta^2\text{-}NO_2)(dppen)_2]$ **6** (Scheme 2). The ^1H NMR spectra of both **5a** and **5b** indicated the presence of hydride with chemical shifts at δ −12.4 and −10.9 respectively. Two phosphorus signals [δ −13.7 and −15.3 (**5a**) and 51.0 and 45.9 (**5b**)] were also recorded in the respective ^{31}P NMR spectra. Such a difference in chemical shift indicates that dppen may adopt different bonding modes in **5a** and **5b**.

The molecular structure of complex **5a** is illustrated in Fig. 5 and important bond lengths and angles are given in Table 6. The three osmium atoms define an irregular triangle with the dppen, NO_2^- ligand and hydride all bridging on the same Os(1)–Os(2) edge [2.896(2) Å]. The dihedral angle between the planes defined by the osmium triangle and the nitrite ligand is 99.7°. The *cis*-1,2-bis(diphenylphosphino)ethylene moiety forms a cyclometallated six-membered ring [Os(1), P(1), C(21), C(22), P(2), Os(2)] in a boat conformation; the bond distance of the central (C=C) in the distorted six-membered ring is 1.39(4) Å, and the average bond angle around P–C–C is 134.5(2)°. The dppen has a clamping function so that a significantly shorter Os(1)–Os(2) distance is observed in contrast to that [2.946(1) Å] in **4**. Unfortunately, we could not obtain suitable crystals of **5b** for X-ray work. It is very tempting to suggest that the dppen ligand is chelating on either Os(1) or Os(2) to form a five-membered ring, if one compared the ^{31}P NMR spectra of **5b** and **6**. However, in the light of the structural similarity of **5a** and **7** but, owing to their very different ^{31}P NMR spectra it is difficult to propose an unambiguous structure for **5b**.

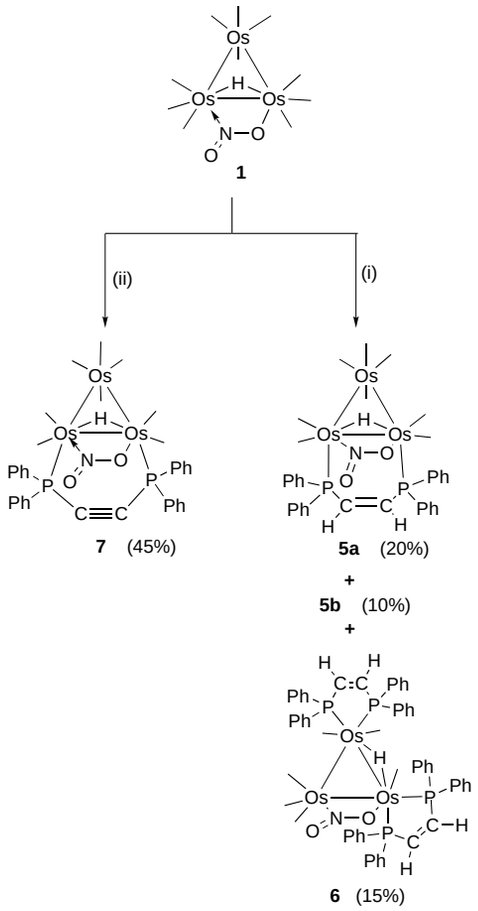

Scheme 2 (i) *cis*-1,2-Bis(diphenylphosphino)ethylene, Me_3NO, CH_2Cl_2 at 40 °C; (ii) bis(diphenylphosphino)acetylene, Me_3NO, CH_2Cl_2 at room temperature

Table 6 Selected bond lengths (Å) and angles (°) for compound **5a**

Os(1)–Os(2)	2.896(2)	Os(1)–Os(3)	2.836(2)
Os(2)–Os(3)	2.856(2)	Os(1)–P(1)	2.344(8)
Os(2)–P(2)	2.337(8)	Os(2)–N	2.12(2)
Os(1)–O(9)	2.15(2)	P(1)–C(21)	1.83(3)
P(2)–C(22)	1.77(3)	C(21)–C(22)	1.39(4)
O(10)–N	1.15(3)	O(9)–N	1.24(2)
Os(1)–Os(2)–Os(3)	59.07(4)	Os(1)–Os(3)–Os(2)	61.16(4)
Os(2)–Os(1)–Os(3)	59.77(4)	Os(1)–Os(2)–P(2)	102.3(2)
Os(1)–Os(2)–N	64.5(7)	Os(2)–Os(1)–O(9)	69.6(5)
Os(2)–Os(1)–P(1)	103.6(2)	Os(1)–P(1)–C(21)	119.0(1)
Os(1)–O(9)–N	105(1)	Os(2)–N–O(10)	119(2)
Os(2)–N–O(9)	120(1)	Os(2)–P(2)–C(22)	118(1)
P(1)–C(21)–C(22)	132(2)	P(2)–C(22)–C(21)	137(2)
O(9)–N–O(10)	120(2)		

Table 7 Selected bond lengths (Å) and angles (°) for compound **6**

Os(1)–Os(2)	2.786(3)	Os(1)–Os(3)	3.031(2)
Os(2)–Os(3)	2.874(3)	Os(1)–P(1)	2.29(1)
Os(1)–P(2)	2.32(1)	Os(3)–P(3)	2.29(1)
Os(3)–P(4)	2.32(1)	Os(1)–O(7)	2.17(3)
Os(2)–N(1)	2.11(4)	P(1)–C(19)	1.85(4)
P(2)–C(20)	1.84(4)	P(3)–C(45)	1.79(3)
P(4)–C(46)	1.89(5)	O(7)–N(1)	1.18(5)
O(8)–N(1)	1.32(6)	C(19)–C(20)	1.33(6)
C(45)–C(46)	1.30(6)		
Os(1)–Os(2)–Os(3)	64.74(7)	Os(1)–Os(3)–Os(2)	56.22(7)
Os(2)–Os(1)–Os(3)	59.04(6)	Os(1)–Os(2)–N(1)	64(1)
Os(2)–N(1)–O(7)	121(3)	Os(2)–Os(1)–O(7)	70.5(7)
Os(1)–O(7)–N(1)	102(2)	Os(2)–N(1)–O(8)	124(2)
P(1)–C(19)–C(20)	117(3)	P(2)–C(20)–C(19)	119(3)
P(3)–C(45)–C(46)	120(3)	P(4)–C(46)–C(45)	117(3)
O(7)–N(1)–O(8)	114(3)		

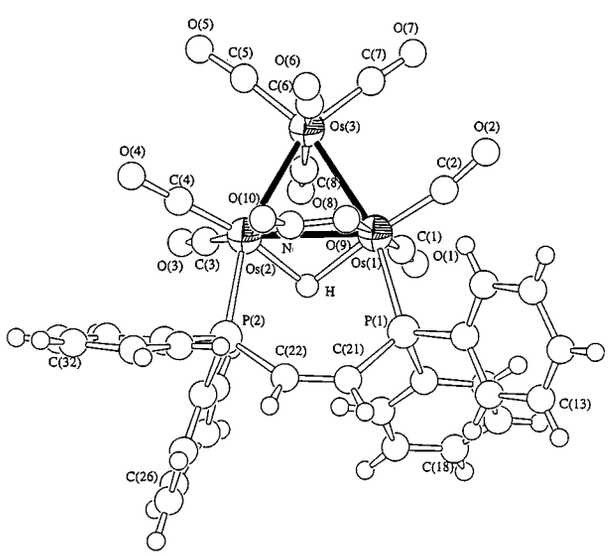

Fig. 5 Molecular structure of $[Os_3(\mu\text{-}H)(CO)_8(\mu\text{-}\eta^2\text{-}NO_2)(dppen)]$ **5a**

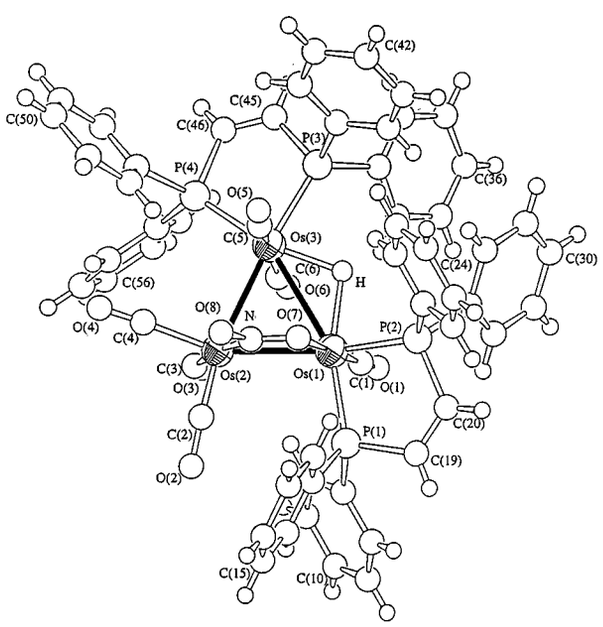

Fig. 6 Molecular structure of $[Os_3(\mu\text{-}H)(CO)_6(\mu\text{-}\eta^2\text{-}NO_2)(dppen)_2]$ **6**

Complex **6** was recrystallised from a *n*-hexane–CH_2Cl_2 solution over a period of 2 d. A perspective view of **6** is depicted in Fig. 6 with principal bond parameters given in Table 7. The Os(1)–Os(3) edge [3.031(2) Å] is much longer than the other Os–Os bonds. This is attributed to the steric requirement between the phenyl rings attached to P(2) and P(3) of the two dppen ligands and also the presence of a hydride bridging across this edge. A multiplet at δ −8.4 was observed in the ^1H NMR spectrum of **6** which can be assigned to this hydride atom. In this context, the hydride has undergone a rearrangement from bridging the Os(1)–Os(2) edge to bridging the Os(1)–Os(3) edge which is uncommon for $[Os_3(\mu\text{-}H)(\mu\text{-}X)(CO)_{10}]$ systems.[22–25] Both dppen ligands behave as a bidentate chelate and form a five-membered ring.

A similar reaction of cluster **1** with a more rigid bidentate phosphine ligand, bis(diphenylphosphine)acetylene (dppa), and Me_3NO afforded a single product $[Os_3(\mu\text{-}H)(CO)_8(\mu\text{-}\eta^2\text{-}NO_2)(dppa)]$ **7** (Scheme 2). The hydride resonance is at

Table 8 Selected bond lengths (Å) and angles (°) for compound **7**

Os(1)–Os(2)	2.905(1)	Os(1)–Os(3)	2.839(1)
Os(2)–Os(3)	2.844(1)	Os(1)–O(9)	2.20(1)
Os(1)–P(1)	2.349(5)	Os(2)–P(2)	2.360(5)
Os(2)–N	2.08(2)	O(9)–N	1.33(2)
O(10)–N	1.17(2)	P(1)–C(21)	1.79(2)
P(2)–C(22)	1.79(2)	C(21)–C(22)	1.17(2)
Os(1)–Os(2)–Os(3)	59.15(3)	Os(1)–Os(3)–Os(2)	61.50(3)
Os(2)–Os(1)–Os(3)	59.35(3)	Os(1)–Os(2)–N	64.8(5)
Os(1)–Os(2)–P(2)	105.9(1)	Os(2)–Os(1)–P(1)	107.0(1)
Os(2)–Os(1)–O(9)	71.3(4)	Os(1)–O(9)–N	99(1)
Os(2)–N–O(10)	129(1)	Os(2)–N–O(9)	129(1)
P(2)–C(22)–C(21)	148(1)	P(1)–C(21)–C(22)	148(1)
O(9)–N–O(10)	106(1)		

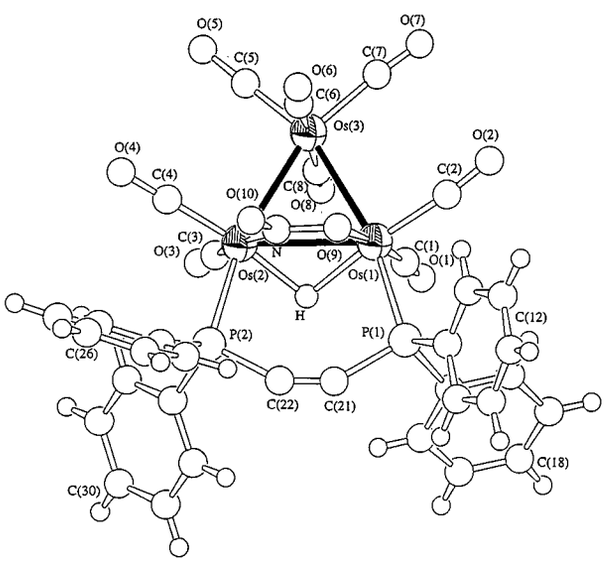

Fig. 7 Molecular structure of $[Os_3(\mu\text{-}H)(CO)_8(\mu\text{-}\eta^2\text{-}NO_2)(dppa)]$ **7**

δ −7.4 and the two phosphorus signals at δ 28.5 and 35.6. Orange crystals of **7** were recrystallised from a *n*-hexane–CH_2Cl_2 solution and the molecular structure was determined by single-crystal X-ray analysis (Fig. 7). Selected bond lengths and angles are given in Table 8. The structure is very similar to that of **5a**. The dppa moiety bridges across the Os(1)–Os(2) edge *via* P(1) [Os(1)–P(1) 2.349(5) Å] and P(2) [Os(2)–P(2) 2.360(5) Å] so that a distorted six-membered ring suffering severe angle strain is formed. The bond length of the central triply bonded carbon in the dppa moiety is 1.17(2) Å which is similar to the average bond length in $[\{Os_3(CO)_{10}(dppa)\}_2]$ [1.18(2) Å].[14] However, the dppa moiety deviates significantly from linearity with the average P–C–C angle 148(1)°. Noticeably, the central ethylene bond angle in **5a** [134.5(2)°] is much smaller than that observed in **7** [148(1)°] and this is probably due to differences in the degree of angular strain in the six-membered ring.

Conclusion

Some triosmium nitrite clusters containing phosphine ligands were prepared and structurally characterised by X-ray crystallography. The clusters **2a** and **2b** contain a labile NMe_3 group that acts as an intermediate for the substitution reactions with phosphine ligands to afford complex **4**. There is no spectroscopic evidence to support the fact that clusters **2a** and **2b** are able to interconvert. Structurally, all the complexes isolated except **6** comprise an osmium triangle with one of the metal–metal edges doubly supported by a hydride and a nitrite moiety. Hydride rearrangement is observed in the highly substituted derivative **6**.

Experimental

Materials and methods

All reactions were carried out under an atmosphere of dry argon using standard Schlenk techniques. Dichloromethane was freshly distilled over calcium hydride prior to use, trimethylamine *N*-oxide was freshly sublimed. All chemicals, except where stated, were from commercial sources (Aldrich and Lancaster) and used as supplied. The nitrite cluster $[Os_3(\mu\text{-}H)(CO)_{10}(\mu\text{-}NO_2)]$ **1** was prepared as described previously.[10] Infrared spectra were recorded on a Bio-Rad FTS-7 spectrometer, NMR spectra on a JEOL GSX 270 Fourier-transform spectrometer with $SiMe_4$ as internal reference and mass spectra on a Finnigan MAT95 instrument by the fast atom bombardment (FAB) technique. Products were separated by thin-layer chromatography (TLC) on silica plates coated with Merck Kieselgel 60 GF254.

Reactions of complex 1

With Me_3NO. Complex **1** (50 mg, 0.055 mmol) was treated with Me_3NO (6 mg, 0.066 mmol) in CH_2Cl_2 (30 cm^3) at room temperature. The mixture was stirred for 1 h and then concentrated under reduced pressure. The products were separated by TLC on silica, with *n*-hexane–CH_2Cl_2 (1:1, v/v) as eluent. Two consecutive bands were eluted (R_f = 0.75 and 0.65 respectively), namely complex **2a** (18 mg, 35%) (Found: C, 15.6; H, 1.1; N, 3.1. Calc.: C, 15.5; H, 1.1; N, 3.0%) and **2b** (10.2 mg, 20%) (Found: C, 15.6; H, 1.2; N, 3.2. Calc.: C, 15.5; H, 1.1; N, 3.0%) of formula $[Os_3(\mu\text{-}H)(CO)_9(\mu\text{-}NO_2)(NMe_3)]$. Orange crystals suitable for single-crystal X-ray analysis were obtained by slow evaporation from a *n*-hexane–CH_2Cl_2 solution at −20 °C.

With PPh_3. Complex **1** (50 mg, 0.055 mmol), PPh_3 (30 mg, 0.114 mmol) and Me_3NO (6 mg, 0.066 mmol) were stirred in CH_2Cl_2 (30 cm^3) at 40 °C for 24 h. The red solution was concentrated under reduced pressure. Separation by TLC on silica, with *n*-hexane–CH_2Cl_2 (1:1, v/v) as eluent, afforded three products. The yellow-orange band product (R_f = 0.75) was complex **3a** (9 mg, 10%) and a second yellow-orange band product (R_f = 0.65) was characterised as the isomeric compound $[Os_3(\mu\text{-}H)(CO)_9(\mu\text{-}NO_2)(PPh_3)]$ **3b** (9 mg, 10%). The third orange product (R_f = 0.3) was characterised as $[Os_3(\mu\text{-}H)(CO)_8(\mu\text{-}NO_2)(PPh_3)_2]$ **4** (30 mg, 40%) and recrystallised from a *n*-hexane–CH_2Cl_2 solution by slow evaporation to give orange-red crystals (Found: C, 38.9; H, 2.3; N, 1.2; P, 4.7. Calc.: C, 38.7; H, 2.3; N, 1.0; P, 4.6%).

With *cis*-1,2-bis(diphenylphosphino)ethylene. Complex **1** (50 mg, 0.055 mmol), dppen (45 mg, 0.113 mmol) and Me_3NO (6 mg, 0.066 mmol) were stirred in CH_2Cl_2 (30 cm^3) at 40 °C for 16 h. The red solution was concentrated under reduced pressure. Separation by TLC on silica, with *n*-hexane–CH_2Cl_2 (4:6, v/v) as eluent, afforded several bands. The yellow product (R_f = 0.7) was recrystallised from a CH_2Cl_2 solution by slow evaporation to give orange crystals of $[Os_3(\mu\text{-}H)(CO)_8(\mu\text{-}NO_2)(dppen)]\cdot CH_2Cl_2$ **5a** (14 mg, 20%), and the second yellow product (R_f = 0.55) **5b** was obtained in low yield (7 mg, 10%). The red product (R_f = 0.35) was recrystallised from a *n*-hexane–CH_2Cl_2 solution by slow evaporation to give red crystals of $[Os_3(\mu\text{-}H)(CO)_6(\mu\text{-}NO_2)(dppen)_2]$ **6** (13 mg, 15%) (Found: C, 44.1; H, 2.9; N, 0.9. Calc. C, 44.1; H, 2.9; N, 0.9%).

With bis(diphenylphosphino)acetylene. An equimolar mixture of complex **1** (50 mg, 0.055 mmol), dppa (22 mg, 0.055 mmol) and Me_3NO (6 mg, 0.066 mmol) was stirred in CH_2Cl_2 (30 cm^3) at room temperature for 16 h. The orange solution was concentrated under reduced pressure. Separation by TLC on silica, with *n*-hexane–CH_2Cl_2 (4:6, v/v) as eluent, afforded a yellow product (R_f = 0.7). It was recrystallised from a *n*-hexane–

Table 9 Summary of crystal data, details of data collection, solution and refinement parameters for compounds **2a**–**7**

	2a	**2b**	**3b**	**4**	**5a**	**6**	**7**
Empirical formula	$C_{12}H_{10}N_2O_{11}Os_3$	$C_{12}H_{10}N_2O_{11}Os_3$	$C_{27}H_{16}NO_{11}Os_3P$	$C_{44}H_{31}NO_{10}Os_3P_2$	$C_{34}H_{23}NO_{10}Os_3P_2{\cdot}0.5CH_2Cl_2$	$C_{58}H_{45}NO_8Os_3P_4$	$C_{34}H_{21}NO_{10}Os_3P_2$
M	928.82	928.82	1132.00	1366.28	1280.57	1578.49	1236.09
Crystal color, habit	Orange, block	Orange, block	Orange, prism	Orange, block	Orange, block	Red, plate	Orange, block
Crystal size/mm	0.32 × 0.32 × 0.34	0.26 × 0.25 × 0.23	0.24 × 0.29 × 0.32	0.25 × 0.25 × 0.29	0.32 × 0.35 × 0.38	0.16 × 0.34 × 0.38	0.21 × 0.23 × 0.32
Crystal system	Monoclinic	Monoclinic	Triclinic	Monoclinic	Monoclinic	Orthorhombic	Triclinic
Space group	$P2_1/c$ (no. 14)	$P2_1/a$ (no. 14)	$P\bar{1}$ (no. 2)	$P2_1/n$ (no. 14)	$C2/c$ (no. 15)	$P2_12_12_1$ (no. 19)	$P\bar{1}$ (no. 2)
a/Å	8.535(4)	12.824(2)	10.408(1)	21.112(2)	33.809(3)	14.316(7)	13.490(5)
b/Å	9.345(3)	10.606(1)	10.760(1)	19.736(2)	11.338(1)	29.51(1)	16.056(5)
c/Å	25.941(3)	16.024(2)	14.585(1)	10.841(1)	26.296(2)	12.772(9)	9.611(4)
α/°	—	—	110.31(2)	—	—	—	103.62(3)
β/°	98.69(2)	108.99(1)	90.08(2)	90.28(2)	129.61(2)	—	110.55(4)
γ/°	—	—	95.89(2)	—	—	—	98.13(3)
U/Å^3	2045(1)	2060.7(5)	1522.5(3)	4517.0(7)	7765(2)	5395(4)	1836(1)
Z	4	4	2	4	8	4	2
D_c/g cm^{-3}	3.016	2.994	2.469	2.009	2.190	1.943	2.236
F(000)	1648	1648	1032	2560	4744	3008	1140
μ(Mo-Kα)/cm^{-1}	186.36	184.96	125.91	85.39	99.92	72.18	104.91
ω Scan width/°	(0.73 + 0.35 tan θ)	(1.52 + 0.35 tan θ)	—	—	—	(0.73 + 0.35 tan θ)	(1.73 + 0.35 tan θ)
Scan speed/° min^{-1}	16	16	—	—	—	16	16
No. reflections collected	3093	3021	6787	23 982	17 299	3251	5056
No. unique reflections	2868	2873	4284	10 750	6196	3251	4809
No. of observed reflections, $I > 3\sigma(I)$	1939	1772	2831	3218	2485	2123	3493
R^a	0.042	0.046	0.041	0.062	0.057	0.060	0.047
R'^b	0.047	0.046	0.043	0.085	0.058	0.068	0.042
Goodness of fit	2.07	2.34	1.33	2.15	1.48	2.22	2.87
Maximum Δ/σ	0.01	0.00	0.04	0.01	0.01	0.09	0.01
No. parameters	128	128	193	266	232	196	202
Maximum, minimum density in ΔF map/e Å^{-3}	1.17, −1.17	1.28, −1.32	1.30, −2.19	2.39, −1.31	2.43, −1.60	2.84, −1.68	1.66, −0.85

^{a} $R = \Sigma \| F_o| - |F_c\|/\Sigma|F_o|$. ^{b} $R' = [\Sigma w(|F_o| - |F_c|)^2/\Sigma wF_o^2]^{\frac{1}{2}}$; $w = 1/[\sigma(F)]^2$.

CH_2Cl_2 solution by slow evaporation to give orange crystals of $[Os_3(\mu\text{-}H)(CO)_8(\mu\text{-}NO_2)(dppa)]$ **7** (30 mg, 45%) (Found: C, 33.1; H, 1.8; N, 1.2; P, 4.9. Calc.: C, 33.0; H, 1.7; N, 1.1; P, 5.0%).

X-Ray crystallography

All pertinent crystallographic data and other experimental details are summarised in Table 9. Intensity data for complexes **2a**, **2b**, **6** and **7** were collected on a Rigaku AFC7R diffractometer and for **3b**, **4** and **5a** on a MAR research image-plate scanner at 298 K using Mo-Kα radiation (λ = 0.710 73 Å) with a graphite-crystal monochromator in the incident beam. The ω–2θ scan technique was employed with a scan rate of 16.0° min^{-1} (in ω) for **2a**, **2b**, **6** and **7**. Three check reflections were monitored periodically throughout data collection and showed no significant variations. All intensity data were corrected for Lorentz-polarisation effects and for absorption by the ψ-scan method.[26] For **3b**, **4** and **5a**, sixty-five 3° frames with an exposure time of 5 min per frame were used. Intensity data were corrected for Lorentz-polarisation effects and for absorption by interimage scaling. The space groups of all crystals were determined from a Laue symmetry check and their systematic absences and confirmed by successful refinement of the structures. For **4**, although the β angle is close to 90 °C, the Laue symmetry is 2/*m* instead of *mmm*. Therefore, a monoclinic system is used. All structures were solved by direct methods (DIRDIF 94)[27] and Fourier-difference techniques. They were refined by full-matrix least-squares analysis with Os and P atoms anisotropic. The Os–Os bridging hydrides for all complexes were located by potential-energy calculations[28] and detailed examination of the ligand arrangements and metal–metal distances. There were some positional disorder problems associated with the phenyl rings in structures **5a**, **6** and **7**. In **6** the phenyl rings were refined as a rigid group with a common thermal parameter. In **7** the phenyl ring involving C(30) exhibits two-fold disorder and was modelled by two sites each with occupancy factor 0.5. However, attempts to refine this phenyl ring were unsuccessful. In **5a** the phenyl ring involving C(26) is positionally disordered. However, attempts to model the disorder by two sites of occupancy failed. All calculations were performed on a Silicon-graphics computer, using the program package TEXSAN.[29]

CCDC reference number 186/808.

Acknowledgements

We thank the Hong Kong Research Grants Council and the University of Hong Kong for financial support. B. K.-M. Hui acknowledges the receipt of a postgraduate studentship, administered by the University of Hong Kong.

References

1 J. Finney, M. A. Hitchman, C. L. Raston, G. L. Rowbottom and A. H. White, *Aust. J. Chem.*, 1981, **34**, 2125.
2 B. F. G. Johnson, A. Silker, A. J. Blake and R. E. P. Winpenny, *J. Chem. Soc., Chem. Commun.*, 1993, 1245.
3 V. Mckee, M. Zvagulis and C. A. Reed, *Inorg. Chem.*, 1985, **24**, 2914.
4 J. A. Halfen, S. Mahapatra, M. M. Olmstead and W. B. Tolman, *J. Am. Chem. Soc.*, 1994, **116**, 2173.
5 A. Chiesa, R. Ugo, A. Sironi and A. Yatsimirski, *J. Chem. Soc., Chem. Commun.*, 1990, 350.
6 F. Oberdorfer, B. Balbach and M. L. Ziegler, *Z. Naturforsch., Teil B*, 1982, **37**, 157.
7 D. A. House, V. Mckee and P. J. Steel, *Inorg. Chem.*, 1986, **25**, 4884.
8 G. Bombiieri, G. Bruno, M. Cusumano and G. Guglielmo, *Acta Crystallogr., Sect. C*, 1984, **40**, 409.
9 V. E. Abashkin, I. G. Fomina, Yu. L. Slovokhotov and Yu. T. Struchkov, *Koord. Khim.*, 1990, **16**, 846.
10 B. K. M. Hui and W. T. Wong, *J. Chem. Soc., Dalton Trans.*, 1996, 2177.
11 M. R. Churchill and B. G. DeBoer, *Inorg. Chem.*, 1977, **16**, 2397.
12 A. J. Deeming, K. I. Hardcastle and S. E. Kabir, *J. Chem. Soc., Dalton Trans.*, 1988, 827.
13 A. J. Deeming, S. Doherty, M. W. Day, K. I. Hardcastle and H. Minassian, *J. Chem. Soc., Dalton Trans.*, 1991, 1273.
14 A. J. Amoroso, B. F. G. Johnson, J. Lewis, A. D. Massey, P. R. Raithby and W. T. Wong, *J. Organomet. Chem.*, 1992, **440**, 219.
15 W. Y. Wong and W. T. Wong, *J. Chem. Soc., Dalton Trans.*, 1995, 2831.
16 A. J. Deeming, S. Donovan-Mtunzi, K. I. Hardcastle, S. E. Kabir, K. Henrick and M. McPartlin, *J. Chem. Soc., Dalton Trans.*, 1988, 579.
17 M. P. Brown, P. A. Dolby, M. M. Harding, A. J. Mathews and A. K. Smith, *J. Chem. Soc., Dalton Trans.*, 1993, 1671.
18 S. R. Hodge, B. F. G. Johnson, J. Lewis and P. R. Raithby, *J. Chem. Soc., Dalton Trans.*, 1987, 931.
19 R. D. Adams, J. E. Babin and H. S. Kim, *Organometallics*, 1987, **6**, 749.
20 R. D. Adams and J. E. Babin, *Organometallics*, 1988, **7**, 963.
21 B. F. G. Johnson, J. Lewis, P. R. Raithby and C. Zuccaro, *J. Chem. Soc., Chem. Commun.*, 1979, 916.
22 R. D. Adams and J. E. Babin, *Organometallics*, 1987, **6**, 1364.
23 R. D. Adams and J. E. Babin, *Organometallics*, 1988, **7**, 2300.
24 R. D. Adams, M. P. Pompeo and J. T. Tanner, *Organometallics*, 1991, **10**, 1068.
25 A. J. Deeming, P. J. Manning, I. P. Rothwell, M. B. Hursthouse and N. P. C. Walker, *J. Chem. Soc., Dalton Trans.*, 1984, 2039.
26 A. C. T. North, D. C. Philips and F. S. Mathews, *Acta Crystallogr., Sect. A*, 1968, **24**, 351.
27 DIRDIF 94, P. T. Beurskens, G. Admiraal, G. Beurskens, W. P. Bosman, R. de Gelder, R. Israel and J. M. M. Smits. The DIRDIF 94 program system, Technical Report of the Crystallography Laboratory, University of Nijmegen, 1994.
28 A. G. Orpen, *J. Chem. Soc., Dalton Trans.*, 1980, 2509.
29 TEXSAN, Crystal Structure Analysis Package, Molecular Structure Corporation, Houston, TX, 1985 and 1992.

Received 21*st October* 1997; *Paper* 7/07588J